Stress Analysis of a Laminated Cylindrical Pipe Subjected to Lateral Compression

Ming Xia, Hiroshi Takayanagi and Kiyoshi Kemmochi

National Institute of Materials and Chemical Research, AIST, MITI
1-1, Higashi, Tsukuba, Ibaraki 305-8565, Japan

ABSTRACT

This paper presents an exact elasticity solution for laminated composite cylindrical pipes under lateral compression. Based on the analytical method, numerical results are obtained for a common thick-walled sandwich pipe. Moreover, the effects of material properties and dimensions on the stresses and radial deflections are also discussed and compared with analytical results obtained from the strain energy. It is shown that the analysis presented is valid for estimating stresses and deflections of thick-walled composite laminated cylindrical pipes subjected to lateral compression.

INTRODUCTION

Recently, there has been a growing interest in developing fiber-reinforced cylindrical composite structures. Thick-walled sandwich pipes made of fiber-reinforced plastics can be used in various applications involving aerospace and offshore endeavors, submarines, pressure vessels, civil engineering structures and others. They can be manufactured to high specific stiffness and strength. The strength of these structures is one of the most important issues. These engineering products can be easily exposed to a variety of temperature and stress fields in different environments. In high-temperature applications, thermal stress may rise above the ultimate strength and lead to unexpected failure. On the other hand, the mechanical behaviors of pipes subjected to external loads (such as internal and external pressures and longitudinal and transverse compressions) are also very important. The longitudinal compressive behavior exhibits shock-load absorption characteristics /1-3/. However, only limited studies have been published dealing with the analysis of fiber-reinforced pipes under lateral compression. Tandon *et al.* /4/ investigated the principal failure modes that take place in the transverse loading of unidirectional brittle matrix composites, such as those with ceramic and glass-ceramic matrices. The failure modes may be matrix cracking, debonding and fiber breakage. The influences of fiber-matrix bond strength and processing-induced residual stresses on damage initiation and ultimate strength were also shown. Alderson and Evans /5/ examined the failure of filament-wound pipes under transverse loading and low-velocity impact using strain gauging and video camera methods. They indicated that the yielding of the resin matrix causes delamination initiation at low load. The failure process then continues with the slow growth of one favorable delamination. Nishiwaki *et al.* /6/ reported on the lateral compressive analysis of a composite cylinder. Based on the quasi-three-dimensional model, the fracture behavior of CFRP cylinders subjected to lateral compressive loading was simulated and compared with experimental results.

At present, the National Institute of Materials and Chemical Research in the Agency of Industrial Science and Technology (AIST) of the Ministry of International Trade and Industry (MITI) is carrying out a study on filament-wound sandwich pipes used for geothermal development. In this paper, we provide an analytical foundation for the investigation of the mechanical properties of composite laminated pipes subjected to lateral compression. Figure 1 contains a schematic

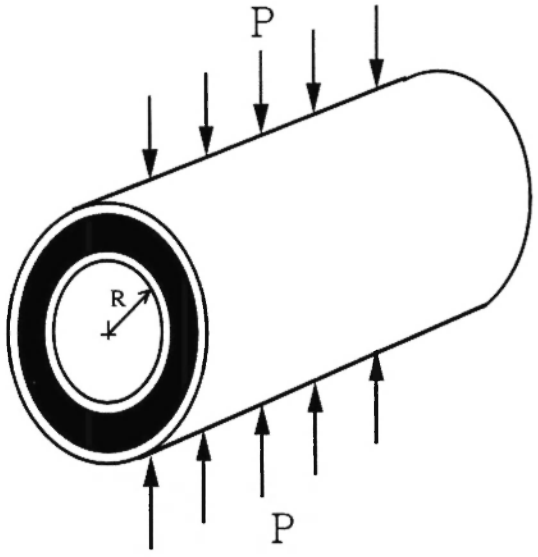

Fig. 1: Sandwich pipe subjected to lateral compression

diagram of lateral compression acting on a composite laminated pipe. Taking a sandwich composite pipe, for instance, the influence of dimensions and material properties on the stress and radial deflection are discussed based on the solution presented. This method is available for use in analyzing deformation and stress in multiple-layered cylinder structures due to lateral compression.

ANALYTICAL PROCEDURE

Bending of a curved beam

Considering a thick-walled curved beam subjected to the bending moment, as shown in Fig. 2, the unit elongation of a thin lamina at a distance y from the middle surface can be written as

$$\varepsilon = \frac{PP_1' - PP_1}{PP_1} = \varepsilon_0 + (\omega - \varepsilon_0)\frac{y}{R+y} \tag{1}$$

where R is the radius of curvature of the middle surface. ε_0 and ω are the strain of the middle surface and the variation of the angle of rotation at the cross-section, respectively, written as

$$\varepsilon_0 = \frac{R'(d\theta + \Delta d\theta) - Rd\theta}{Rd\theta} \qquad \omega = \frac{\Delta d\theta}{d\theta} . \tag{2}$$

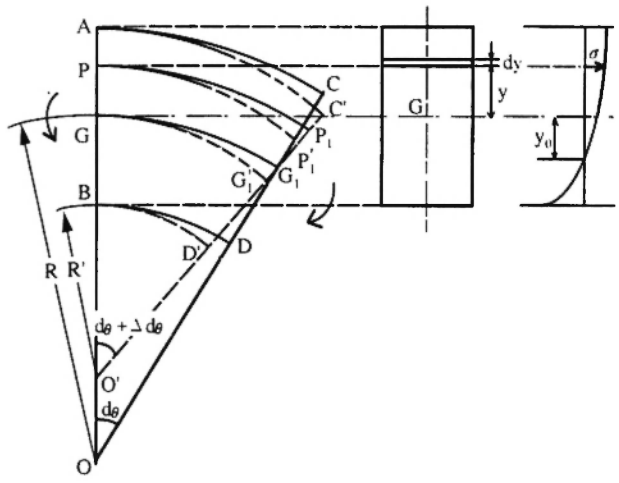

Fig. 2: Curved beam subjected to bending moment

For a curved composite beam, the stress, the axial force and the moment acting on the beam can be expressed, respectively, as follows:

$$\sigma_i = E_i\left\{\varepsilon_0 + (\omega - \varepsilon_0)\frac{y}{R+y}\right\}(i = 1,2,\cdots,n), \tag{3}$$

$$N = \sum_{i=1}^{n}\int_{A_i}\sigma_i dA_i = \sum_{i=1}^{n}\int_{A_i}E_i\left\{\varepsilon_0 + (\omega - \varepsilon_0)\frac{y}{R+y}\right\}dA_i \tag{4}$$

and

$$M = \sum_{i=1}^{n}\int_{A_i}\sigma_i y dA_i = \sum_{i=1}^{n}\int_{A_i}E_i\left\{\varepsilon_0 + (\omega - \varepsilon_0)\frac{y}{R+y}\right\}y dA_i \tag{5}$$

If $\int_{A_i} y dA_i = I_i$ and $\int_{A_i}\frac{y}{R+y}dA_i = -k_i A_i$, we get

$$\int_{A_i}\frac{y^2}{R+y}dA_i = -I_i + Rk_i A_i. \tag{6}$$

k_i and I_i are defined as the section modulus of a curved beam and the first moment of area, respectively, which are given in Appendix A. Substituting these expressions for Eqs. (4) and (5), the axial force (N) and the moment (M) can be given by the following:

$$N = \varepsilon_0\sum_{i=1}^{n}E_i A_i - (\omega - \varepsilon_0)\sum_{i=1}^{n}k_i E_i A_i \tag{7}$$

and

$$M = \varepsilon_0 \sum_{i=1}^{n} E_i I_i + (\omega - \varepsilon_0) \sum_{i=1}^{n} (E_i I_i + Rk_i E_i A_i) . \quad (8)$$

ε_0 and ω can be obtained from Eqs (7) and (8), written as

$$\varepsilon_0 = \frac{N \sum_{i=1}^{n} (E_i I_i + Rk_i E_i A_i) + M \sum_{i=1}^{n} k_i E_i A_i}{\left(\sum_{i=1}^{n} E_i A_i \right) \left(\sum_{i=1}^{n} (E_i I_i + Rk_i E_i A_i) \right) + \left(\sum_{i=1}^{n} E_i I_i \right) \left(\sum_{i=1}^{n} k_i E_i A_i \right)} \quad (9)$$

and

$$\omega = \frac{NR \sum_{i=1}^{n} k_i E_i A_i + M \sum_{i=1}^{n} (k_i E_i A_i + E_i A_i)}{\left(\sum_{i=1}^{n} E_i A_i \right) \left(\sum_{i=1}^{n} (E_i I_i + Rk_i E_i A_i) \right) + \left(\sum_{i=1}^{n} E_i I_i \right) \left(\sum_{i=1}^{n} k_i E_i A_i \right)} \quad (10)$$

The solutions of strain and stress can be found by substituting Eqs. (9) and (10) into Eqs. (1) and (3), respectively.

The strain ε_0 of the middle surface is not equal to zero even if the axial force is zero. It is known that the radius of curvature of the neutral surface does not coincide with that of the middle surface. The position of the neutral surface y_0, shown as Fig. 2, can be derived from $\sigma_i = 0$. We get

$$y_0 = \frac{-R \left(N \sum_{i=1}^{n} E_i I_i + (NR + M) \sum_{i=1}^{n} k_i E_i A_i \right)}{M \sum_{i=1}^{n} E_i A_i + (NR + M) \sum_{i=1}^{n} k_i E_i A_i} . \quad (11)$$

For a curved beam with a ratio of curvature to beam thickness over 10, the axial force (N) can be ignored compared to the moment (M). The position of the neutral surface is given by

$$y_0 = \frac{-R}{1 + \sum_{i=1}^{n} E_i A_i \Big/ \sum_{i=1}^{n} k_i E_i A_i} . \quad (12)$$

Moment and deformation of pipe under lateral compression

Let us consider a laminated composite pipe compressed by two forces P acting along a diameter. Figure 3 shows the analysis of the forces on a quarter pipe. Denoting the bending moment at section C by M_0, we find that the moment (M) at any cross-section (m-n) is

$$M = \frac{PR}{2}(1 - \cos\phi) - M_0 \quad (13)$$

where R is the radius of curvature of the middle surface.

The axial force (N) at any cross-section (m-n) is given by

$$N = \frac{P}{2}\cos\phi . \quad (14)$$

The bending moment (M_0) can be determined from the condition of symmetry. The angle of rotation of the cross-section between $\phi = 0$ and $\phi = \pi/2$ remains at a right angle after deformation due to the acting force P. Because there is no variation in the angle of rotation at cross-section C, we have

$$\int_0^{\pi/2} \omega d\phi = 0 . \quad (15)$$

Substituting Eqs. (13) and (14) for Eq. (10) and using Eq. (15), we get

$$M_0 = \frac{PR}{\pi}\left(\frac{\pi}{2} - 1 + \alpha_D \right) \quad (16)$$

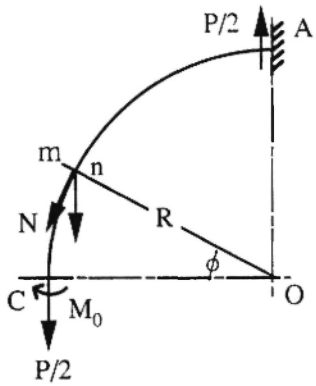

Fig. 3: Analysis of forces acting on pipe

where α_D is the parameter related to the thickness of laminated composite pipes, given by

$$\alpha_D = \frac{\sum_{i=1}^{n} k_i E_i A_i}{\sum_{i=1}^{n} (k_i E_i A_i + E_i A_i)}. \quad (17)$$

The influence of the bending moment (M) on the angle of rotation of the cross-section is much larger than that of the axial force (N) when the thickness of the pipe is much less than the radius of curvature of the middle surface. In this case, the parameter α_D is close to zero.

The radial deflections of the cross-section with $\phi = 0$ and $\pi/2$ can be given by

$$u|_{\phi=0} = \int_0^{\pi/2} \varepsilon_0 R(1-\sin\phi)d\phi + \int_0^{\pi/2} \alpha R \sin\phi d\phi$$
$$u|_{\phi=\pi/2} = \int_0^{\pi/2} \varepsilon_0 R\cos\phi d\phi + \int_0^{\pi/2} \alpha R\cos\phi d\phi \quad (18)$$

Substituting Eqs. (9) and (10) for Eq. (18), the lengthening (u_L) and the shortening (u_S) of diameters at $\phi = 0$ and $\phi = \pi/2$ (along the direction of the acting force) are given by

$$u_L = \frac{(PR/2)\left(R(\pi-3)\sum_{i=1}^{n} E_i A_i + \pi R\sum_{i=1}^{n} k_i E_i A_i + \sum_{i=1}^{n} E_i I_i\right) - M_0 R\left(\pi\sum_{i=1}^{n} k_i E_i A_i + (\pi-2)\sum_{i=1}^{n} E_i A_i\right)}{\left(\sum_{i=1}^{n} E_i A_i\right)\left(\sum_{i=1}^{n} (E_i I_i + R k_i E_i A_i)\right) + \left(\sum_{i=1}^{n} E_i I_i\right)\left(\sum_{i=1}^{n} k_i E_i A_i\right)} \quad (19)$$

and

$$u_S = \frac{-(PR/4)\left(R(4-\pi)\sum_{i=1}^{n} E_i A_i - \pi\sum_{i=1}^{n} E_i I_i\right) + 2M_0 R\sum_{i=1}^{n} E_i A_i}{\left(\sum_{i=1}^{n} E_i A_i\right)\left(\sum_{i=1}^{n} (E_i I_i + R k_i E_i A_i)\right) + \left(\sum_{i=1}^{n} E_i I_i\right)\left(\sum_{i=1}^{n} k_i E_i A_i\right)} \quad (20)$$

When the thickness of the pipe is much less than the radius of curvature of the middle surface, the lengthening (u'_L) and shortening (u'_S) of the diameters can be obtained from the strain energy theory, given by

$$u'_L = \frac{PR^3}{2\overline{EI}}\left(\frac{4}{\pi} - 1\right) \text{ and } u'_S = \frac{PR^3}{4\overline{EI}}\left(\pi - \frac{8}{\pi}\right) \quad (21)$$

where $\overline{EI}$ is the equivalent bending rigidity, which is given in Appendix B.

The analytical errors of the lengthening and shortening of the diameters between the thick curved beam and strain energy theories are

$$\delta_L = \left|\frac{u_L - u'_L}{u_L}\right| \text{ and } \delta_S = \left|\frac{u_S - u'_S}{u_S}\right|. \quad (22)$$

RESULTS AND DISCUSSION

This analytical procedure is applied to an example of a sandwich composite pipe. Table 1 lists the material constants and dimensions of the sandwich pipe. The pipe has an inner radius (r_0) of 50mm, a core-layer thickness (t_c) of 20 mm and a skin-layer thickness (t_s) of 2 mm. In the present study, the first and third skin layers (inner layer and outer layer) of the sandwich pipe are made of the same material. The stress analysis of the sandwich pipe is carried out under a lateral compressive force of 1MN/m. The elastic moduli of the skin layers and the core layer are 80GPa and 5GPa, respectively.

The lengthening and shortening of diameters on a pipe with $\phi = 0°$ and 90° are listed in Table 2. The radial deflections at $\phi = 0°$ and 90° are 0.657mm and –0.906 mm, respectively. Error analysis shows a deviation of

Table 1
Material constants and dimensions of the sandwich pipe

	Young's Modulus (GPa)	Thickness (mm)
Skin (t_s)	80	2
Core (t_c)	5	20
Inner radius (r_0)	50mm	
Compressive force (P)	1MN/m	

Table 2
Lengthening and shortening of diameters with $\phi = 0°$ and 90°

Theory	$\phi = 0°$	$\phi = 90°$
	(mm)	
Curved beam	0.657	−0.906
Strain energy	0.772	−0.841
Error (%)	17.5	7.2

Minus stands for the shortening of diameter

17.5% and 7.2% at $\phi = 0°$ and 90°, respectively, based on the curved beam and the strain energy theories.

Figures 4 and 5 show the stress distributions through the wall of the sandwich pipe at sections C and A, respectively. The skin layers are subjected to much higher stresses compared to the core layer.

The stress distributions of the inner and outer pipes are shown in Fig. 6. The inner surface of the sandwich pipe is subjected to compressive-to-tensile stresses when the angle ϕ varies from 0° to 90°, while the outer surface is subjected to tensile-to-compressive stresses. The inner and outer surfaces of the sandwich pipe with section A have maximum tensile and maximum compressive stresses, respectively. Therefore, it is safe to predict that the first failure mode for the sandwich pipe will occur on section A. Figure 7 shows the position of the neutral surface of the pipe at different cross-sections. It has been found that the position of the

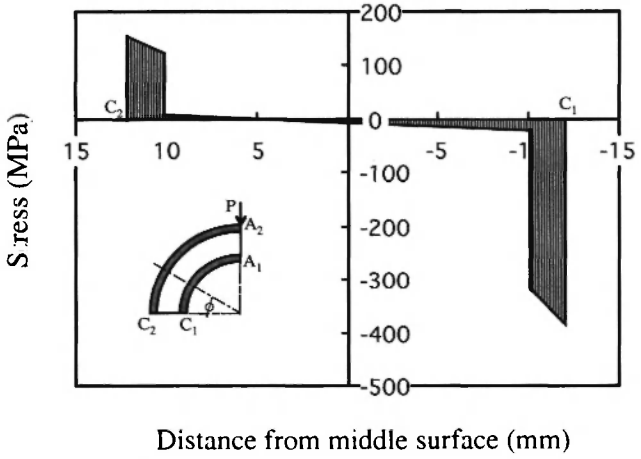

Fig. 4: Stress distribution within sandwich pipe with section C

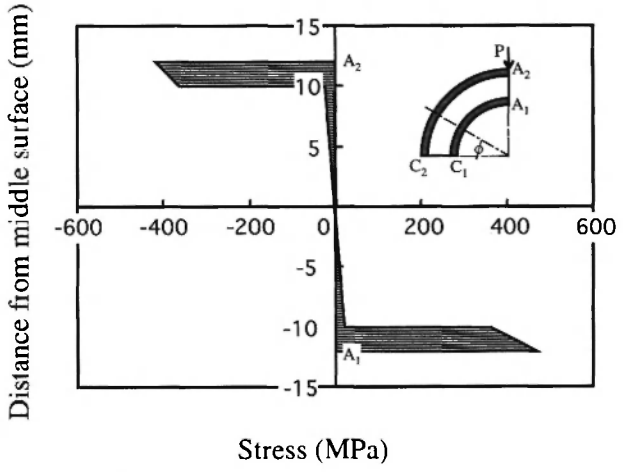

Fig. 5: Stress distribution within sandwich pipe with section A

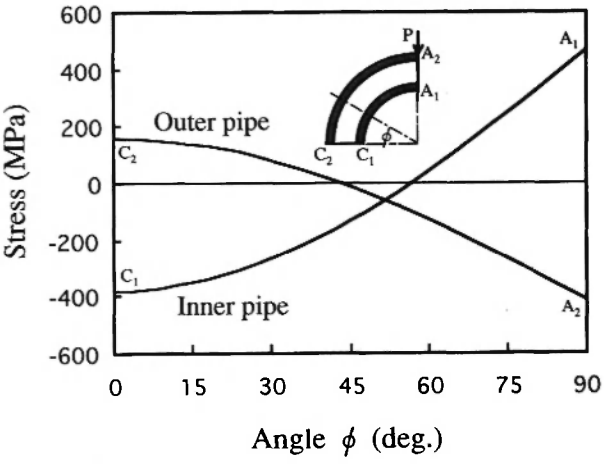

Fig. 6: Stress distributions within sandwich pipe at the inner and outer pipes

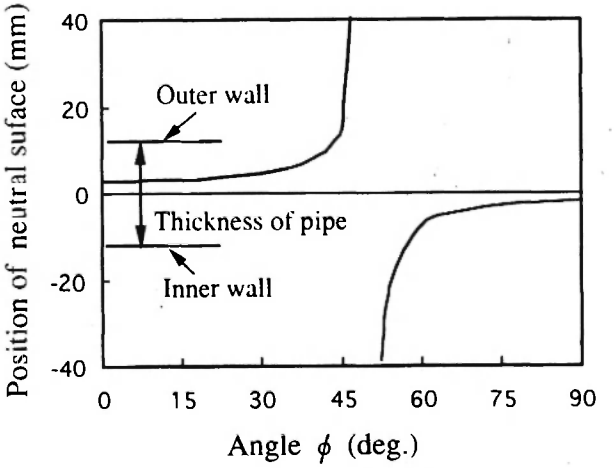

Fig. 7: Position of neutral surface with pipe

neutral surface varies with the angle ϕ. The position of the neutral surface is beyond the thickness of the sandwich pipe when the angle ϕ ranges from about 43° to 57°.

For a sandwich with a skin thickness of 2 mm, the relationship between the thickness of the core layer and the radial deflections of sections with $\phi = 0°$ and 90° is shown in Fig. 8. The variation of the radial deflection with the core thickness is shown to be nonlinear. The radial deflections rapidly increase as the core thickness decreases.

The influence of the modulus ratio between the core and skin layers on the stresses of the pipe at sections A and C is shown in Fig. 9. The stresses are almost proportional to the modulus ratio. Both tensile and compressive stresses at the inner and outer pipes tend to decrease slightly when the modulus ratio of core-to-skin layers increases because the deformation of the pipe decreases as the core stiffness increases. The core material with a high stiffness intensifies the transfer of the force from the inner to outer layers.

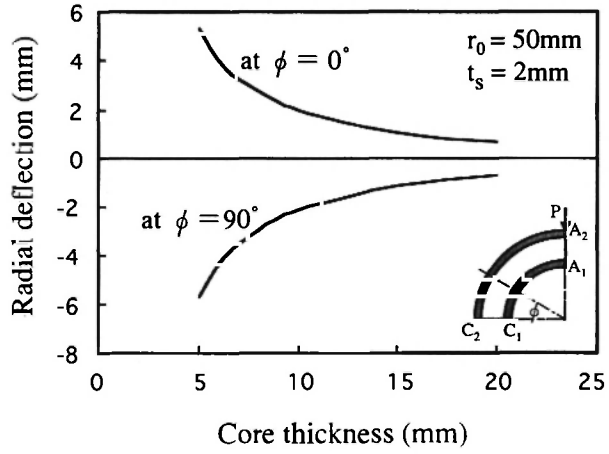

Fig. 8: Variation of the radial deflection of pipe with the core thickness

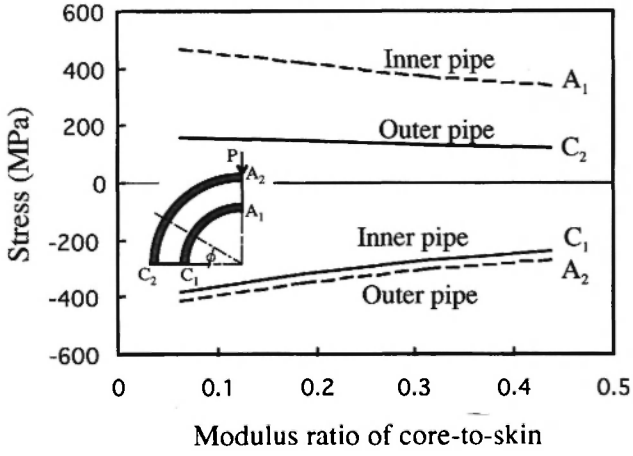

Fig. 9: Relationship between the stress and the modulus ratio of core-to-skin layers

Based on the thick curved beam and the strain energy theories, the errors for the radial deflections of the sandwich pipe are analyzed. Figure 10 shows the error analysis of the radial deflections with respect to the core thickness of the sandwich pipe with a skin thickness of 2mm. The analysis shows that the error values increase as the thickness of the core layer increases. The error values of the radial deflection at $\phi = 0°$ are larger than those at $\phi = 90°$. The error values of the radial deflections at $\phi = 90°$ are as high as 18% when the thickness-to-radius ratio (t_c / r_0) is about 40%.

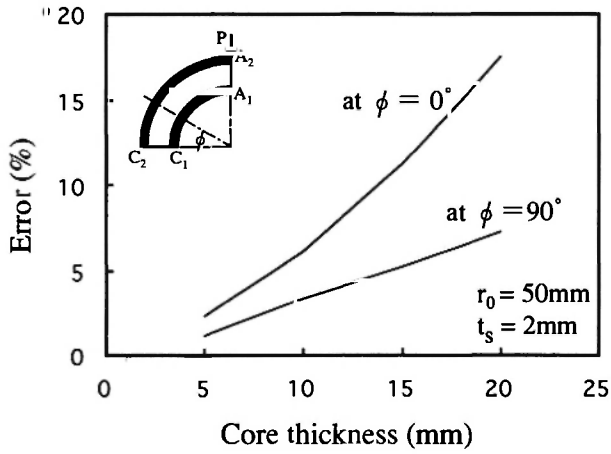

Fig. 10: Error analysis of the radial deflection with respect to the core thickness

CONCLUSIONS

Through application of the curved beam theory, an exact solution is presented for analyzing the lateral compression of laminated thick-walled cylindrical pipes. Stress and deformation analyses of the sandwich composite pipe are performed using the exact solution.

The radial deflections are shown to be nonlinear with core thickness and rapidly increase as the core thickness decreases.

In an analysis of the radial deflection of pipes with thick walls, a significant difference is revealed between the curved beam and the strain energy theories.

ACKNOWLEDGEMENT

Dr. M. Xia acknowledges the financial support received from the New Energy and Industrial Technology Development Organization (NEDO).

APPENDIX A

With reference to Fig. A-1, the section modulus of a curved beam can be written as

$$k_i = \frac{R}{r_i - r_{i-1}} \ln\left(\frac{r_i}{r_{i-1}}\right) - 1 \quad (i = 1,2,\cdots,n) \qquad \text{(A1)}$$

where t_i and r_i are the thickness and the radius, respectively, of the curvature at the ith layer.

The first moment of area of the curved beam can be given by

$$I_i = \frac{(R - r_i)^2 - (R - r_{i-1})^2}{2} \quad (i = 1,2,\cdots,n). \qquad \text{(A2)}$$

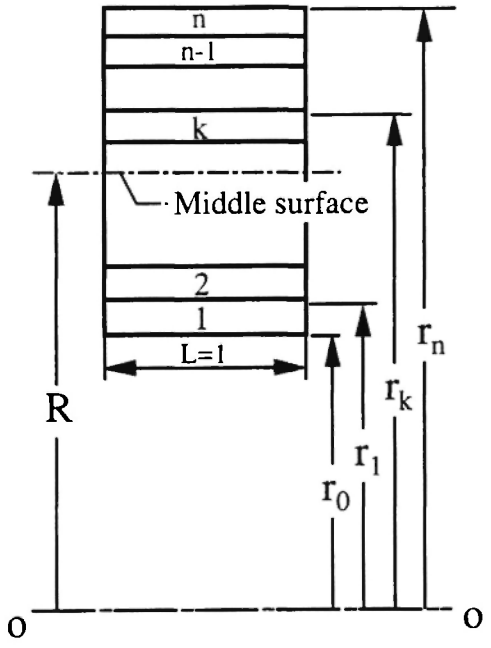

Fig. A-1: Laminate cross-section

APPENDIX B

The equivalent bending rigidity $\overline{EI}$ is obtained from

$$\overline{EI} = \sum_{i=1}^{n} E_i\left(t_i^3/12 + y_i^2 t_i\right) \qquad \text{(B1)}$$

where E_i and t_i are the longitudinal modulus and the thickness of the ith layer, respectively. y_i is the distance from the middle surface, written as

$$y_i = \bar{\eta}_i - \bar{\eta}, \; t_i = r_i - r_{i-1} \quad (i = 1,2,\cdots,n) \qquad \text{(B2)}$$

and

$$\bar{\eta}_1 = \frac{t_1}{2}, \quad \bar{\eta}_i = \sum_{k=1}^{i-1} t_k + \frac{t_i}{2} \quad (i = 2,3,\cdots,n). \qquad \text{(B3)}$$

When the thickness of the pipe is much less than the radius of curvature of the middle surface, the thickness may be ignored compared with the radius of curvature of the middle surface. $\bar{\eta}$ can be expressed by

$$\bar{\eta} = \sum_{i=1}^{n} \bar{\eta}_i E_i A_i \Big/ \sum_{i=1}^{n} E_i A_i \,. \qquad \text{(B4)}$$

REFERENCES

1. H. Hamada, J.C. Coppola, D. Hull, Z. Maekawa and H. Sato. Comparison of energy absorption of carbon/epoxy and carbon/PEEK composite tubes, *Composites*, **22**, 245-252 (1992).
2. T. Katayama, K. Imadegawa and T. Hirai. Analysis of fracture mechanism of FW ring under impact load, *Proc. 71st JSME Fall Annual Meeting* (Japanese), **930-63**A, 106-108 (1993).
3. T. Hirai, A. Yokoyama, Y. Murata and Y. Mutoh. Fracture behavior under impact lateral compression in filament-wound composites, *Materials (Japanese)*, **35**, 515-520 (1986).

4. G.P. Tandon, R.Y. Kim and R E. Dutton. Failure modes in unidirectional composites under transverse loading, *Journal of Reinforced Plastics and Composites*, **16**, 33-49 (1997).
5. K.L. Alderson and K.E. Evans. Failure mechanisms during the transverse loading of filament-wound pipes under static and low-velocity impact conditions, *Composites*, **23**, 167-173 (1992).
6. T. Nishiwaki, A. Yokoyama, Z. Maekawa, H. Hamada and S. Mori. A quasi-three-dimensional lateral compressive analysis method for a composite cylinder, *Composite Structures*, **32**, 293-298 (1995).